The ν_4 Band of FNO$_2$

Charles J. Miller[1] and Stanley P. Sander

Jet Propulsion Laboratory, California Institute of Technology

Mail Stop 183-901, 4800 Oak Grove Drive, Pasadena, CA 91109-8099

[1] National Research Council/NASA Jet Propulsion Laboratory Research Associate

[2] email cmiller@mldws.jpl.nasa

Number of Pages: 20

Number of Figures: 4

Number of Tables: 2

Proposed Running Head: The V₄ Band of ... 7C

Please send proofs to

    Dr. Charles J. Miller

    Jet Propulsion Laboratory

    Mail Stop 183-901

    4800 Oak Grove Drive

    Pasadena CA 91109-8099

Abstract

We report the first high resolution infrared spectra of nitryl fluoride NO_2 The intense v_4 band associated with the NO_2 antisymmetric stretching vibration, has been observed in the 750 - 825 cm region The spectrum displays extensive rotational structure and consists solely of b-type transitions C_e 500 infrared and 51 microwave transitions have been fit to generate rotational constants for th v_4 state $(v_0$ 793.46684 cm and improved constants for the ground state. Rotationally resolved infrared line positions are now available for the identification of NO_2, an atmospheric product of ClO and ClO oxidation.

INTRODUCTION

This paper continues the series of reports from our laboratory on the high resolution spectroscopy of oxyhalide and NO_x compounds (1 ,2 ,3) implicated in atmospheric ozone depletion (4). High resolution spectra enable one to determine important structural and bonding properties for these molecules, many of which are unstable. Rotationally resolved line positions can be used to monitor the concentrations of these molecules in atmospheric remote sensing experiments such as ATMOS (5) or in laboratory measurements of reaction kinetics (6).

Nitryl fluoride, FNO_2, has been known as a reactive laboratory compound since the 1930's (7), but has not been the subject of many investigations. It is now known to be one of the principal end products of chlorofluorocarbon oxidation (8). Similar oxidation pathways should exist for the HFC replacement gases, therefore it is important to investigate the spectroscopy and kinetics of FNO_2. We have demonstrated that FNO_2 is the sole product of the $F + NO_2$ reaction (9) in contrast to the $Cl + NO_2$ reaction where both the $ClNO_2$ and $ClONO$ structural isomers are formed. Additionally, FNO_2 and its structural isomer FONO are computationally challenging molecules: their bonding, structure and physical properties have been the focus of intense theoretical interest (10).

Microwave spectroscopy on FNO_2 has provided precise ground state rotational constants (11 ,12 ,13 ,14) and a molecular structure (12), but only low resolution infrared spectra have been reported (15 ,16 ,17). During work on the $F + NO_2$ reaction system

initiated to obtain high resolution spectra of the ONO isomer we identified infrared

features due to (57) cm^{-1}), ν_6 (762 cm^{-1}), ν_2 (82 cm^{-1} ν_1 (3 2 cm) and ν_4

1794 cm^{-1}) bands of ONO$_2$. All five regions yielded extensive rotational structure when

investigated under high resolution Here we present a full rotational analysis of the

intense absorption band corresponding to ν_4, the NO$_2$ antisymmetric stretching vibration.

EXPERIMENTAL

The spectra were recorded on a Bomen DA8-3 Fourier transform spectrometer

optically coupled to a fast-flow/multipass absorption cell (2,3). A liquid helium cooled

GeCu detector (Infrared Laboratories) and custom amplifier provided the interferogram

signal. This apparatus was designed for the study of transient molecules and has sufficient

pumping capacity to reduce the residence time within the 5 meter long cell to 00

milliseconds while maintaining a total press re of 0 Torr. The system also contains a

dedicated OMA (EG&G Princeton Applied Research) to monitor reaction diagnostics via

UV/Visible absorption.

Nitryl fluoride was produced by the reaction of fluorine atoms with N 2

$$ F + NO_2 \rightarrow FNO_2 $$

fluorine atoms were produced in a microwave discharge cavity and combined with N 2

and helium buffer gas in a high pressure pre-reactor region The reaction mixture

flowed from the pre-reactor into the lower pressure region of the multipass absorption cell for observation. Optimal reaction conditions were determined by monitoring the decay 01 the NO_2 absorption signal in the 300 400" nm region and the concurrent growth of the FNO_2 absorption in the 80 - 240 nm range (18). Under conditions of excess F atoms, any NO_2 introduced into the system was quantitatively converted into FNO_2. The UV spectra showed no indication of further reaction o the FNO_2 product with F atoms to regenerate NO_2 or to produce F NO. It was hoped that the F -l NO_2 system would also produce FONO, by analogy to the reaction of Cl -l NO_2, but neither the strong 17 15 cm^{-1} band nor any other absorptions attributable to FONO were observed (9). Survey spectra recorded at i .0 cm^{-1} resolution over the 600 2500 cm^{-1} range revealed strong absorptions centered at 822, 13 12, and 1794 cm^{-1} and a sharp, comparatively weak feature near 762 cm^{-1}, in excellent agreement with previous reports of the FNO_2 band positions from low resolution work (16,J7). The reaction conditions could easily be manipulated to saturate the absorptions at 822, 1312, and 1 '/(M cm^{-1}. A (lc.tailed account of the F-4NO_2 reaction may be found in Reference 9.

Spectra of the v_4 band were recorded with a resolution of 0,005 cm^{-1} and boxcar apodization using a I 600" - 1850 cm^{-1} band pass filter (OCl J). 128 scans were co-added to obtain the final spectrum. The NO_2 concentration in the reaction mixture was limited so that the strongest features in the spectrum absorbed less than 50%. Infrared line positions were determined using the Kitt Peak peak finder algorithm (19) and calibrated using H_2O transitions (?0) present in the spectrum due to the small amount of residual

water vapor in the optical path. All line positions were assigned an experimental uncertainty of 0.001 cm^{-1}.

SPECTRAL ANALYSIS

FNO$_2$ is an oblate rotor with C$_{2v}$ symmetry and moderate asymmetry: $\kappa = 0.504$ (11,12,13). The presence of two indistinguishable ^{16}O nuclei, each having zero nuclear spin, requires that the molecular wavefunction follow Bose-Einstein statistics and that the rovibrational component of the wavefunction must have even parity with respect to the molecular a-axis (see Figure 1). The vibrational symmetry of the ground state is a$_1$, therefore only even K$_a$ values have non-zero spin-statistical weights. The $\nu_4 = 1$ state has b$_1$ vibrational symmetry so that only odd K$_a$ values have non-zero spin-statistical weights in this state. This results in a pure b-type infrared spectrum since all transitions must have $\Delta K_a = \pm 1$. The ν_4 overview spectrum in Figure 2 exhibits the weak Q branch pattern characteristic of b-type bands.

All spectral calculations were carried out using Pickett's SPFIT and SPCAT programs (21). Ground state spectroscopic constants were calculated from the 51 microwave transitions reported in References 12, 13, and 14 using Watson's S-reduced Hamiltonian (22)

$$H_{rot} = \frac{1}{2}(B^{(S)}_x + B^{(S)}_y)P^2 + [B^{(S)}_z - \frac{1}{2}(B^{(S)}_x + B^{(S)}_y)]P_z^2 + \frac{1}{2}(B^{(S)}_x - B^{(S)}_y)(P_+^2 + P_-^2)$$

$$- D_J P^4 - D_{JK} P^2 P_z^2 - D_K P_z^4 + d_1 P^2 (P_+^2 + P_-^2) + d_2 (P_+^4 + P_-^4)$$

in the III^r representation. The results are presented in Table 1. The microwave data set contained 39 lines with J ≤ 15, K$_a$ ≤ 10 and 10 lines with 6 ≤ J ≤ 29, (ΔX$_a$ ≤ 20. Each line was assigned (.05 MHz uncertainty. Two lines from the ultra high precision FTMW work of Styger et al. (14) were included with 5 kHz uncertainties. This set of ground state constants was sufficiently accurate that it was assumed to predict rotational energy levels for J" = 0-70 with negligible uncertainty

A preliminary simulation of the ν$_4$ spectrum was performed assuming the rotational constants for the ν$_4$ = 1 state were identical to those of the vibrational ground state. This calculation produced a spectrum which was qua itatively similar to the one we observed: the P- and R-branches were dominated by clusters of low K$_a$" transitions and there was no central Q-branch. Transition sequences having constant K$_a$" were identified using the interactive Loomis-Wood fitting program LWS1 developed by the Giessen group (23) Initially, 300 transi ons between 775 and 1815 cm^{-1} with J" = 20 40 were assigned and the assignments ver fied using ground state combination differences. Good estimates of C' and (A' +) for the ν$_4$ = 1 state were also determined using combination differences.

Successive fitting iterations involved re-optimizing the spectroscopic constants, assigning additional lines based on the predicted line positions and intensities, and then repeating the process. In this manner, 1539 infrared transitions were incorporated into the final line list. The quantum numbers of the infrared transitions span the range $J''= 0-65$, $K_a''= 0-40$, and $K_c''= 0-65$, thus ensuring an excellent determination of all quartic centrifugal distortion constants. Assigned lines deviating more than 2.5 times the experimental uncertainty from their calculated positions were rejected from the fit. The final constants for the ground state (Table 1) and $v_4= 1$ (Table 2) were determined from a simultaneous fit of the combined microwave and infrared data sets. Ground state and $v_4= 1$ constants were also determined using Watson's A-reduced Hamiltonian; these values are collected in Table 2.

DISCUSSION

1. The Ground State

There have been several previous investigations of the FNO_2 ground vibrational state using microwave spectroscopy In 1952 Smith and Magnuson (1 1) identified 8 rotational transitions and deduced that the molecule possessed a planar C_{2v} structure. In 1968 Legon an d Millen (12) determined a substitution structure for FNO_2 after observing 1 7 rotational transitions in the 17 - 33 GHz region for each of three isotopomers: $F^{14}N^{16}O_2$, $F^{15}N^{16}O_2$, and $F^{14}N^{18}O^{16}O$ The $F^{14}N^{18}O^{16}O$ spectrum was particularly interesting since the asymmetric substitution of the oxygen atoms destroyed the C_2

symmetry axis and previously forbidden transitions were observed. This study improved the precision of the A, B, and C rotational constants by three orders of magnitude, but the analysis was constrained to transitions with $J \leq 15$ and neglected centrifugal distortion. Later that year, Mirri et al. ("13) determined the four in-plane centrifugal distortion constants from 33 transitions measured in the 100 - 140 GHz region. $^1NO_2$ spectroscopy then remained dormant until the recent ultra-high resolution FTMW measurements of Styger et al. (14). which were used to determine the ^{14}N and ^{19}F nuclear hyperfine constants.

The rotational constants determined in the present study are collected in Table 1 along with the results of Legon and Millen (12) and Mirri et al. (13). The different sets of constants agree very Well. The slightly larger A, B, and C values determined by Legon and Millen probably result from the neglect or centrifugal distortion corrections. The fact that the rotational constants we derived from all 51 of the measured microwave transitions are essentially the same as those derived by Mini et al. supports this collusion.

W C . have converted the centrifugal distortion constants reported by Mirri et al. (13) from the $\tau_{\alpha\beta\gamma\delta}$ form into the corresponding S-reduced Hamiltonian constants using Watson's relationships (24 ,25). The agreement between these values and those derived in the present work is quite good. The IR transitions improve the statistics of the fit without substantially altering the values of the centrifugal distortion constants, even though the IR data set includes transitions up to $J'' = 65$, $K_a'' = 40$ while the microwave data

are limited to maxima of $J''=29$, $K_a''=20$. The fina set of groun state constants are all well-determined and exhibit arameter/1σ erroi atios in excess of 800:1. The itting Hamiltonian was also expanded to included sextic centrifugal distortion constants; however, since these constants failed to improve the fit, the Iamiltonian was imited to quar ic centrifugal distortion ter ns.

2. The $\nu_4=1$ State

The appearance of the ν_4 band is qualitatively similar to the ν_2 NO_2 antisymmetric stretching band of INO_3 (26). Intense and R-branch transitions dominate he spectrum with regular transition clusters occurring a about 42 cm⁻¹ intervals. Each cluster consists of a series of lines which converge to a head at he low wavenumber limit of the cluster. The lowest wavenum e feature in each cluster is he most intense, usually containing several overlapping transitions. Rotational analysis shows that each cluster represents a constant 2 ''·$\mathbf{x}_c$ value. Beginning with he head of each cluster, the transitions originate from ground state vibrational levels with the quantum numbers $N_{0,N}$, $N_{2,N-2}$, $N_{2,N-4}$, $N_{3,N-6}$, etc. where $N=2J''-K_c''$. The strongest line wi hin each cluster has $K_c''=J''$ and the line strengths di inisl as $J''-K_c''$ increases ine absolute J assignments for each cluster were confir ned using ground state con ination differences.

Figure 3   P-branch clusters for $2J''-K_c''$ values of 4   40, and 39 beginning with he transitions $40_{1,40} \leftarrow 4_{0,4}$ (775.4389 cm⁻¹), $39_{1,39} \leftarrow 4_{0,40}$ (1775.8992 cm⁻¹)

and $38_{1,38} \leftarrow 39_{0,39}$ (1776.3582 cm^{-1}), respectively. The spin-statistical weights of the ground and $v_4=1$ states ensure that only b-type transitions occur, as mentioned above. Since many transitions are "missing" from the spectrum, individual features are easily resolved. The concentration of transitions near the low wavenumber head of each cluster is clearly evident.

There are other strong absorptions which run through the P- and R-branch regions and are unrelated to the $2J''$-K_C'' $\approx N$ clusters. These transitions are characterized by single lines having about 0.40 cm^{-1} spacings. They continue to have appreciable intensity even in the far wings of the spectrum where the $2J$ -$K_C = N$ clusters are weak ($N > 60$). These lines are due to transitions originating in K_a'' J'', K_C''=0 levels. Many of these lines derive their intensity from the overlap of two nearly degenerate transitions. The transitions $19_{17,3} \leftarrow 20_{18,2}$, $19_{17,3} \rightarrow 18_3$ 1775.6761 cm^{-1}), and $18_{1,2} \leftarrow$ 9_{18}, $8_{7,1} \leftarrow$ $19_{18,2}$ (1776.2942 cm^{-1}) marked A and B in Figure W, are of this type. Including these transitions in the fit refined the centrifugal distortion constants D_K D_{JK}, D_K' D_{JK}, " and d_2 and reduced correlations between all of the $v_4=1$ constants.

The Q-branch region between 1790 and 1800 cm^{-1} is much more congested than the P- or R-branch regions. A portion of the Q-branch is shown in Figure 4. The higher line density and uncertainty as to absolute J values prohibited assignment of these lines during the early phases of the fitting process. However, the Q-branch line positions and intensities were accurately predicted once the rotational constants from fitting the P- and

R-branch regions were available. The Q-branch lines were then incorporated into the fit. This resulted in a further refinements 01 the centrifugal distortion constants and an overall reduction in the 1σ values for the V_4 1 constants.

The fitting residuals are statistically distributed and no detectable perturbations are observed in the spectrum. This is in agreement with our calculations, which predict no other levels within -100" cm^{1} of the 1793.466841 cm^{1} v_4 origin. The harmonic frequency $\omega_4 = 1789$ cm^{1} calculated by Lee at the $CCSD(T)/TZ2P$ level of theory (10c) compares favorably with the observed fundamental vibrational frequency. The FNO_2 NO_2 antisymmetric stretching fundamental is significantly higher than the corresponding frequencies observed for HNO_3 (1709.56746 cm^{1} (26)) and $ClNO_2$ (1683.894022 cm^{1} (27)), the good agreement between experiment and theory concerning both the frequency and relative intensity of v_4 suggests that there is nothing unusual about the bonding in FNO_2. The high frequency of this NO_2 antisymmetric stretching frequency implies that the F atom is withdrawing appreciable electron density from the NO_2 group to form $F^{\delta-}$ $NO_2^{\delta+}$. Recently, Styger et al (14) concluded that in FNO_2 the F atom withdraws 0.36 of an electron from the half-filled NO_2 $6a_1$ orbital, thus providing quantitative verification of the electron redistribution.

Given the asymmetry of FNO_2, one would normally express the spectroscopic constants within the framework of Watson's A-reduced Hamiltonian. We have performed fits using this Hamiltonian and found the quality of the fits comparable to

those obtained using the S-reduced Hamiltonian (Table 2). We note, however, that Δ_K is

an order of magnitude smaller than expected and that δ_K is an order of" magnitude larger

than expected. The ratio $\delta_K/\Delta_k = 6.3$ is unphysical and represents optimized fitting

parameters rather than reasonable molecular behavior. Therefore, we have included the

A-reduced constants in Table only for the sake of comparison with similar molecules;

the S- reduced constants are our preferred values

CONCLUSIONS

We have reported the first rotationally resolved infrared spectrum of FNO_2. Over

1500 transitions in the intense v_4 band have been assigned. Well-defined rotational and

quartic centrifugal distortion constants have been determined for the ground and $v_4= 1$

vibrational states and these constants reproduce the experimental line positions with an

rms error Of 0.00078 cm^{-1}. The high frequency of the NO_2 anti symmetric stretching

vibration, $v_0 = 1793.46684$ I cm^{-1}, implies significant redistribution of electron density

from the NO_2 moiety onto the F atom to form a partially ionic F^δ $NO_2^{\delta'}$ structure.

However, the small changes in rotational constants upon excitation into the $v_4= 1$ state and

the ability of high-quality ab initio calculations to reproduce the v_4 vibrational frequency

suggest no unusual bonding in FNO_2. The v_4 band provides an excellent opportunity for

molecule-specific detection of FNO_2 since the strongest individual lines coalesce near the

low wavenumber heads of transition clusters in the P- and R- branches to form even more

intense features while still maintaining nearly Doppler-limited linewidths. Analysis of the other vibrational fundamentals is in progress.

ACKNOWLEDGMENTS

REFERENCES

1. M. Birk, R. R. Friedl, E. A. Cohen, H. M. Pickett, and S. P. Sander, *J. Chem. Phys.* **91**, 6588-6597 (1989).

2. V I. Lang, S. P. Sander, and R. R. Friedl, *J. Mol. Spectrosc.* **132**, 89-103 (1988).

3. S Höjer, R. D. May, and C. E. Miller, *J. Quant. Spectrosc. Radiat. Transfer* **55**, 273-278 (1996).

4. Scientific Assessment of Ozone Depletion: 1994, WMO GlobalOzoneResearch and Monitoring Project, Report No. 37, 1994.

5. M. R. Gunson, M. M. Abbas, M. C Abrams, M. Allen, L. R. Brown, T. L. Brown, A Y. Chang, A. Goldman, F. W. Irion, L.L. Lowes, E. Mahieu, G. L. Manney, H. A.

Michelsen, M. J. Newchurch, C. P. Rinsland, R. J. Salawitch, G. P. Stiller, G. C. Toon, Y. L. Yung, and R. Zander, submitted to *Geophys. Res. Lett.*

6. T. S. Dibble, M. M. Maricq, J. J. Szente, and J. S. Francisco, *J. Phys. Chem.* **99**, 17394-17402 (1995).

7. R. Schmutzler, *Angew. Chem.* **80**, 466-481 (1968); *Angew. Chem. Internat. Edit.* **7**, 440-455 (1968).

8. M. M. Maricq, J. J. Szente, T. S. Dibble, and J. S. Francisco, *J. Phys. Chem.* **98**, 12294-12304 (1994).

9. C. E. Miller and S. P. Sander, submitted to *J. Phys. Chem.*

10 a) T. J. Lee and J. E. Rice, *J. Chem. Phys.* **97**, 4223-4232 (1992) and references therein; b) T. S. Dibble and J. S. Francisco, *Chem. Phys. Lett.* **215**, 423-426 (1993); c) T. J. Lee, *Chem. Phys. Lett.* **216**, 194-199 (1993).

11. D. F. Smith and D. W. Magnuson, *Phys. Rev.* **87**, 226-227 (195?).

12. A. C. Legon and D. J. Millen, *J. Chem. Soc. A* **1968**, 1736-1740 (1968).

13. A. M. Mirri, G. Cazzoli, and 1. Ferretti, *J. Chem. Phys.* 49, 2775-2780 (1968).

14. C. Styger, B. Gatehouse, N. 1 Ieineking, W. Jäger, and M . C. L. Gerry, *J. Chem. Soc. Faraday Trans.* **89**, 1899- 19(v (**1 993**).

15. R. E. Dodd, J. A. Rolfe, and L. A. Woodward, 'f *rans. Far. Soc.* 52, 145- 15 I (1 956).

16. 11. L. Bernitt, R. 11. Miller, and I. C. Hisatsune, *Spectrochim. Acta* **23A**, ?37-248 (1967).

17. K. O. Christie, C. J. Schack, and R. D. Wilson, *Inorg. Chem.* **13**, 28 11-2815 (1974).

18. A. P. Uthman, G. A. Sherman, and (i. A. Takacs, *Spectrochim. Acta* **34A**, I 109- I 110 (1978).

19. 1.. R. Brown, J. S. Margolis, R t 1. Norton, and B. D. Stedry, *Appl. Spectrosc.* 37, 287-292 *(1983)*.

20 R. A. Toth, *J. Opt. Soc. Am.* B 8, ? 236-2255 (I 99 I).

2 I H. M. Pickett, *J. Mol. Spectrosc.* 148, 371-377 (199 I).

22. J. K. G. Watson, *J. Chem. Phys.* 48, 451 ʔ 4528 (1968).

23. B. 1'. Winnewisser, J. Reinstädtler, K. M. '1'. Yamada, and J. Behrend, *J. Mol. Spectrosc.* 136, I 2-16 (1 989); F. Stroh, *Thesis,* **Justus-**] iebig Universität Giessen (1991).

24. **W.** Gordy and R. 1.. ('(ink, *Microwa ve Molecular Spectra,* Chapter 8, Wiley Interscience/New York, 1984.

25 1.1 Iedberg and 1. M. Mills, *J. Mol. Spectrosc.* 160, 11 '/- 142 (1993).

26. A. G. Maki, *J. Mol. Spectrosc.* 127, 1 04 111 (1988).

27 J, Orphal, M. Morillon-Chapey, and G. Guelachvili, .1. *Mol. Spectrosc.* 165, 315-322 (1994).

LIST OI1' TABLES

TABLE 1

FNO$_2$ Ground Vibrational State Spectroscopic Constants in the S-reduction[a]

	Ref. 13	Ref. 13	This work	This work
A	0.440 350 7 (27)	0.440 340 5 (27)	0.440 347 892 (107)	0.440 347 908 0 (274)
B	0.381 808 7 (27)	0.381 805 8 (27)	0.381 805 757 (76)	0.381 805 842 8 (220)
C	0.204 109 4 (27)	0.204 107 5 (27)	0.204 107 646 (64)	0.204 107 703 (23)
$D_J/10^{-7}$		5.495 8[b]	5.494 23 (454)	5.496 27 (127)
$D_{JK}/10^{-7}$		-8.978 2[b]	-8.989 09 (317)	-8.986 72 (147)
$D_K/10^{-7}$		4.043 8[b]	4.060 38 (604)	4.057 57 (220)
$d_1/10^{-7}$		-0.809 39[b]	-0.800 19 (230)	-0.801 78 (250)
$d_2/10^{-7}$		0.278 42[b]	0.276 39 (163)	0.277 46 (317)
rms		30 MW	49 MW, 2.5 MW	49 MW, 2.5 MW, 15 IR

[a] All values expressed in cm^{-1}. Numbers in parentheses after each constant reflect the 1σ error in units of the last digit.

[b] The quartic centrifugal distortion constants given in Ref. 13 are (in MHz):

$$\tau_{aaaa} = -0.039814 \pm 0.000456$$

$$\tau_{bbbb} = -0.078638 \pm 0.000087$$

$$\tau_{aabb} = 0.012452 \pm 0.000375$$

$$\tau_{abab} = -0.048868 \pm 0.000115$$

These values have been converted into the spectroscopic constants for the S-reduction using the appropriate relationships (24,25).

TABLE 2

Spectroscopic Constants for the FNO_2 Ground and $v_4=1$ States[a,b]

S-reduced Hamiltonian		A-reduced Hamiltonian	
A''	0.440 347 968 6 (274)	A''	0.440 348 811 2 (327)
B''	0.381 805 842 8 (220)	B''	0.381 804 456 2 (310)
C''	0.204 107 703 (23)	C''	0.204 107 964 (26)
$D_J''/10^{-7}$	5.496 27 (127)	$\Delta_J''/10^{-7}$	4.928 3 (47)
$D_{JK}''/10^{-7}$	-8.986 72 (147)	$\Delta_{JK}''/10^{-7}$	-5.617 6 (237)
$D_K''/10^{-7}$	4.057 57 (220)	$\Delta_K''/10^{-7}$	1.249 (20)
$d_1''/10^{-7}$	-0.801 781 (450)	$\delta_J''/10^{-7}$	0.808 19 (260)
$d_2''/10^{-7}$	0.277 46 (317)	$\delta_K''/10^{-7}$	-7.920 8 (494)
$A'-A''$	-0.002 843 52 (45)	$A'-A''$	-0.002 843 35 (51)
$B'-B''$	-0.000 186 62 (44)	$B'-B''$	-0.000 186 62 (56)
$C'-C''$	-0.000 654 576 (153)	$C'-C''$	-0.000 654 496 (157)
$(D_J'-D_J'')/10^{-9}$	-2.371 (129)	$(\Delta_J'-\Delta_J'')/10^{-9}$	1.194 (273)
$(D_{JK}'-D_{JK}'')/10^{-9}$	3.956 (237)	$(\Delta_{JK}'-\Delta_{JK}'')/10^{-9}$	-17.15 (102)
$(D_K'-D_K'')/10^{-9}$	-0.928 (149)	$(\Delta_K'-\Delta_K'')/10^{-9}$	16.67 (81)
$(d_1'-d_1'')/10^{-9}$	2.381 (159)	$(\delta_J'-\delta_J'')/10^{-9}$	-2.405 (195)
$(d_2'-d_2'')/10^{-9}$	-1.712 (75)	$(\delta_K'-\delta_K'')/10^{-9}$	17.28 (217)
v_0	1793.466 841 (70)	v_0	1793.466 816 (75)
rms error	0.000 78	rms error	0.000 79

[a] All values expressed in cm^{-1}. Numbers in parentheses after each constant reflect the 1σ error in units of the last digit.

[b] All constants determined from the data set consisting of 49 MW, 2 FTMW and 1511 IR transitions
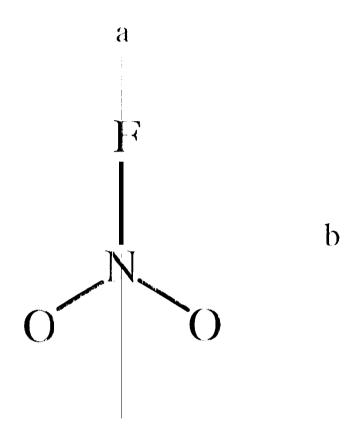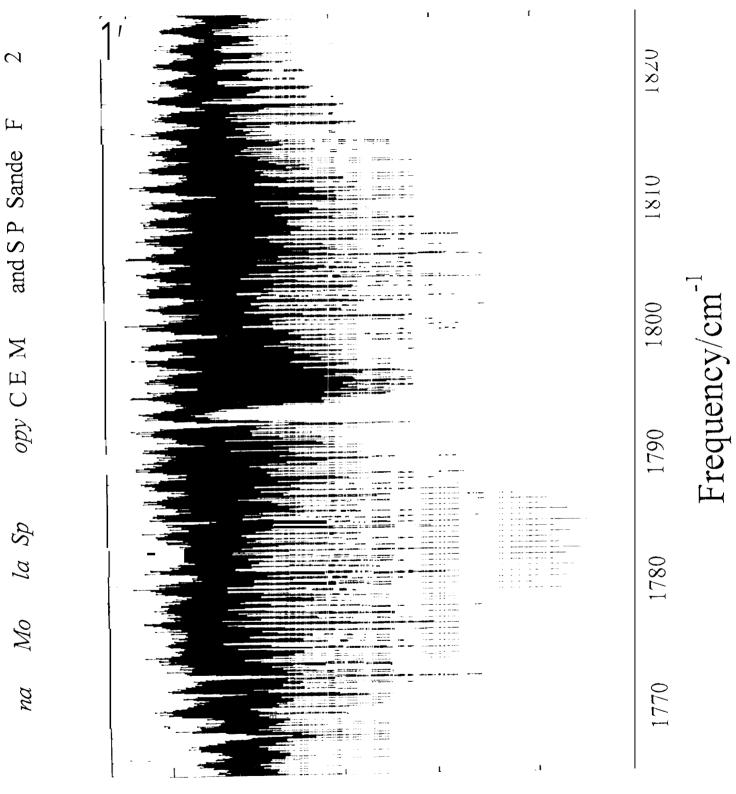
FIGURE CA ''IONS

Figure 1 The molecular structure of FNO_2 shown superi iposed on he molecular axes. The c-axis is perpendicular to the page. R_{N1} 146.7 pm, R_N 17.98 pm, $O_{ONO} = 36°$ (Re : 2

Figure 2. An overview of the v_4 spectrum recorded at 0.005 cm^{-1} resolution.

Figure 3. An expanded view of several $2J' - k_c'' = N$ clusters and two high K_a'' lines in the v_4 P-branch. See the text for details.
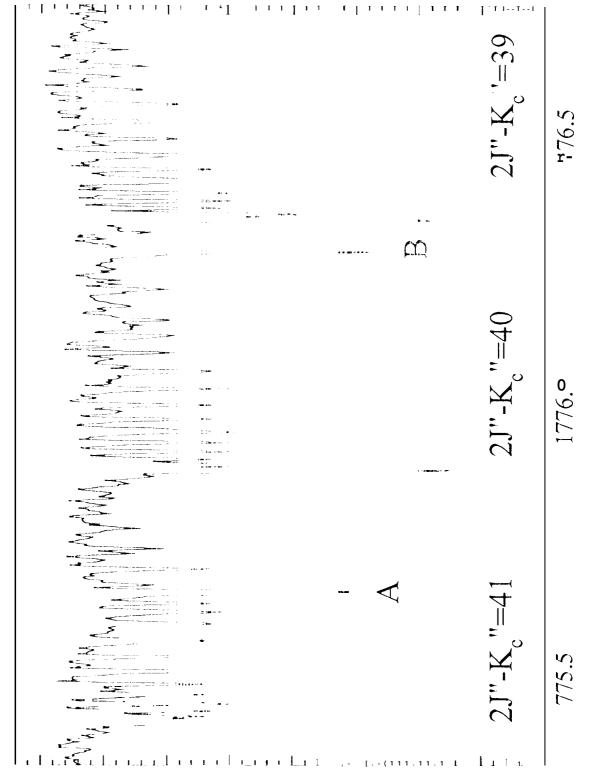
Figure 4. A detailed view of the v_4 spectrum near the vibrational origin.

a

F

b

N

O   O

na   Mo   la Sp   opy C E M   and S P Sande   F   2

Absorption/arb. units

Frequency/cm^{-1}

1770   1780   1790   1800   1810   1820

Absorption/arb. units

Frequency/cm^{-1}

775.5
1776.0
1776.5

$2J''-K_c''=41$
$2J''-K_c''=40$
$2J''-K_c''=39$

A
B

Journal of Molecular Spectroscopy; C. E. Miller and S. P. Sander, Figure 4.

Absorption/arb. units

Frequency/cm^{-1}

1794.5   1795.0   795.5   1796.0

LIST OF SYMBOLS

Symbol	Definition
A, B, C	Principal rotational constants
A'', B'', C''	Principal rotational constants for the lower state in a specified transition
$A', \ldots$	Principal rotational constants for the upper state in a specified transition
$\Delta_K, \Delta_{JK}, d_1, d_2$	Quartic centrifugal distortion constants in the S-reduction
$\Delta_K, \Delta_J, \Delta_{JK}, \delta_J, \delta_K$	Quartic centrifugal distortion constants in the A-reduction
$\tau_{\alpha\beta\delta}$	Distortion constant for the angular momentum operator $P_\alpha P_\beta P_\gamma P_\delta$
$\tau_{aaaa}, \tau_{bbbb}, \tau_{aabb}, \tau_{abab}$	Axis specific quartic centrifugal distortion constants
ν_0	Origin of a vibrational transition